NANO REVIEWS

COACTION PUBLISHING

Review Article

Probing and controlling fluorescence blinking of single semiconductor nanoparticles

Hsien-Chen Ko[1,2,3], Chi-Tsu Yuan[1]* and Jau Tang[1,4]*

[1]Research Center for Applied Sciences, Academia Sinica, Taipei, Taiwan; [2]Molecular Science and Technology Program, Taiwan International Graduate Program, Institute of Atomic and Molecular Sciences, Academia Sinica, Taipei, Taiwan; [3]Department of Chemistry, National Tsing Hua University, Hsinchu, Taiwan; [4]Institute of Photonics, National Chiao-Tung University, Hsinchu, Taiwan

Received: 5 December 2010; Revised: 11 January 2011; Accepted: 12 January 2011; Published: 11 February 2011

Abstract

In this review we present an overview of the experimental and theoretical development on fluorescence intermittency (blinking) and the roles of electron transfer in semiconductor crystalline nanoparticles. Blinking is a very interesting phenomenon commonly observed in single molecule/particle experiments. Under continuous laser illumination, the fluorescence time trace of these single nanoparticles exhibit random light and dark periods. Since its first observation in the mid-1990s, this intriguing phenomenon has attracted wide attention among researchers from many disciplines. We will first present the historical background of the discovery and the observation of unusual inverse power-law dependence for the waiting time distributions of light and dark periods. Then, we will describe our theoretical modeling efforts to elucidate the causes for the power-law behavior, to probe the roles of electron transfer in blinking, and eventually to control blinking and to achieve complete suppression of the blinking, which is an annoying feature in many applications of quantum dots as light sources and fluorescence labels for biomedical imaging.

Keywords: *single molecule*; *confocal microscopy*; *quantum dot*; *nanoscience*; *fluorescence intermittency*; *blinking*; *electron transfer*; *Auger relaxation*

During the past 20 years, there has been tremendous progress in the developments of nanofabrication and high resolution imaging techniques in order to fabricate and to explore the structures and physical properties of nano-sized materials such as quantum dots (QDs), nanorods (NRs), quantum wells, quantum wires, and nanotubes. These recent developments have generated wide interest among researchers from many disciplines, and it has opened a new realm of

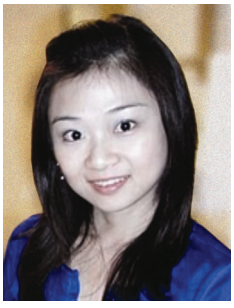

Hsien-Chen Ko is currently a PhD student in Molecular Science and Technology of Taiwan International Graduate Program (TIGP) in Academia Sinica. Her research interests include electron transfer and blinking mechanism of nanoparticles using single-molecule spectroscopy under supervision of Professor Tang.

Chi-Tsu Yuan, a post-doctor of Prof. Tang's group, received his Ph.D. degree in electro-physics from National Chiao Tung University in Taiwan in 2008. His research focuses on nano-photonics, including single-molecule spectroscopy, exciton-photon coupling, and nano-plasmonics.

Jau Tang, an APS Fellow, received Ph.D. degree from University of California at Berkeley. He was a researcher at Argonne National Laboratory, Bell Laboratories, and a senior scientist at California Institute of Technology. He is now a research fellow and a former associate director of the Research Center for Applied Sciences, Academia Sinica in Taiwan. He is a senior editor of Nano Reviews, a board director of Asian Nanoscience and Nanotechnology Association, and the chairman of its Taiwan's chapter. His research interests include photoluminescence and ultrafast phenomena of nanomaterials.

Citation: Nano Reviews 2011, **2:** 5895 - DOI: 10.3402/nano.v2i0.5895

scientific research (1–3) hotly pursued by scientists and engineers in many countries with constant large inflow of grants from their governments. Since these semiconductor nanoparticles possess unusual optical and electrical properties, they have been demonstrated in novel utilizations offering potential applications in many areas in science and technology. For example, QDs possess size-dependent photoluminescence and high quantum-yield, therefore, QDs are utilized as biological labels for cancer cells (4). Moreover, one could tune the band-gap emission of these QDs, which has a very narrow line width and large optical oscillator strength. These QDs have offered many potential applications including new types of lasers, electro-optical modulators, and high density logical devices. In addition, with chemical manipulations, large-scale nano-assemblies could be fabricated bottom-up from colloidal QDs whose sizes are easily controlled.

Blinking, or more formally called intermittency, is a very interesting phenomenon frequently observed in confocal microscopy of single molecules or single nanoparticles at low concentration. Such intriguing behavior is not exclusive only for nano-sized particles, intermittency has been observed much earlier in the macroscopic world. Such phenomenon often involves non-linear dynamic systems including geomagnetic field reversal of the earth, sun spot activities, and also the response from a non-linear electronic circuit near Hopf bifurcation point (5). Even with long standing history of the observation of intermittency in the macroscopic world, fluorescence blinking in the nano-world has drawn much attention in the last decade, primarily due to the advance and easy access of confocal microscopy. With these confocal techniques, researchers could observe photoluminescence of a single molecule or a single nanoparticle by zooming into a micron-size area of a highly dispersed sample. There are several advantages for single particle/molecule spectroscopy. In particular, it avoids the complication due to sample heterogeneity and conformational variations among an ensemble system. Consequently, it offers useful information that is not readily available in the measurement of an ensemble system.

To explain the role of electron transfer reaction and the blinking mechanism of QDs, several explanations were proposed (6–16). The observation of blinking in single QDs was first reported by Nirmal and coworkers (17). They illuminated single QDs with light continuously observing that some QDs went dark abruptly and became light again (17). A few years later, Kuno et al. discovered the waiting time distribution of the on-off (light-dark) events followed an unusual power-law distribution (18). In addition, the exponent of the inverse power law was found to be close to 1.5. One of the popular models is the diffusion-controlled electron transfer (DCET) model (19) proposed by Tang and Marcus (20). They explained the roles of photoinduced spectral diffusion and electron transfer reactions between the neutral light state and the positively charged dark state as the underlying mechanisms for the fluorescence blinking in QDs. They also addressed the intricate relationship between power-law intermittency of single QDs and the ensemble-averaged fluorescence decay that follows a quasi-stretched exponential behavior. To account for the observed deviation from 1.5 power-law exponent for some experiments, they proposed a more general diffusion-controlled electron transfer model in the presence of non-Debye dielectric medium, as well as extending from the ideal Debye medium.

Ever since the first observation of blinking phenomena of QDs by Nirmal et al. (17), there is a fast growing wealth of literature on experimental and theoretical studies of the unusual behavior. On the experimental side, several groups have made significant improvements in the understanding of the blinking phenomena such as Nirmal et al. (17), Krauss et al. (21, 22), Nirmal et al. (23), Empedocles and Bawendi (24), Shimizu et al. (25, 26), Chung and Bawendi (27), Fisher et al. (28), Chung et al. (29), Kuno et al. (18, 30, 31), Messin et al. (32), Brokmann et al. (33), Verberk et al. (34), Verberk and Orrit (35), Cichos et al. (36), Issac et al. (37), and many others (38–41). Some more recent developments could be found in a review (42). In addition to the observation of blinking Nirmal et al. (17, 23), Krauss and Brus (21) also identified the dark state as a positively charged hole residing inside the core of a QD while an electron possibly is trapped elsewhere. Kuno et al. (18) first reported the $t^{-3/2+\alpha}$ power-law behavior, where α is a small number for the waiting time distribution for both light and dark events. In a later study (30), they eliminated an earlier model assuming a static distribution of the electron/hole trapping sites. Empedocles and Bawendi (24) then linked the intermittency to photo-induced spectral diffusion, and they suggested a possible role of diffusion for the cause of the power-law behavior. In another study, they observed two emission tracks with energy separated by $20 \sim 25$ meV for QDs spin-coated on a rough gold surface (26). Their results indicated that the dark charged state on a quartz substrate might become emissive when single QDs were coated on a rough gold surface due to plasmonic effects by the gold substrate. They also noted that the histogram of such binary jumps between two traces of emission wavelengths also followed a $t^{-3/2}$ power law. Chung and Bawendi explored the relationship between ensemble fluorescence decay (27) and single QDs intermittency. Brokmann and coworkers (34) demonstrated the use of QDs as biological labels and as single photon sources. Intensity correlation techniques

Citation: Nano Reviews 2011, 2: 5895 - DOI: 10.3402/nano.v2i0.5895

were used in Verberk et al. (34) and Verberk and Orrit (35) and they observed similar $t^{-3/2+\alpha}$ power-law behavior. Correlation between the dielectric property of the trapped state and the power-law behavior was studied by Cichos et al. (36), Issac et al. (37). Haase et al. (43) and Schuster et al.'s group (44) observed a similar power-law behavior in single organic chromophores indicating that the power-law behavior in fluorescence blinking is not restricted only to QDs.

On the theoretical development side, understanding of the blinking mechanisms and power-law blinking statistics has been advanced by many groups since the work by Tang and Marcus (20, 50, 51), Efros and Rosen (45), Wang and Wolynes (46), Boguna et al. (47), Barkai et al. (48), Margolin and Barkai (49), and Frantsuzov and Marcus (52). They considered a rate equation among three states with 0, 1, and 2 electron-hole pairs to describe random telegraph signaling or blinking. This model led to an ordinary exponential decay instead of power law. Wang and Wolynes (46) used a reaction diffusion scheme to describe Poisson statistics of intermittency in single molecules, but the issues regarding QDs and power-law behavior were not discussed. Barkai et al. (48) studied the Lévy flight model and its connections to power-law behavior. Kuno et al. (31) used a static model with exponentially distributed distances for the tunneling rate. However, this model requires an unreasonable surface trap site over an extremely large distance distribution to accommodate seven to eight decades for the dynamic range of blinking statistics. Shimizu et al. (25) described a discrete-time random walk process for the dark state in resonance with the excited QDs. Verberk et al. (34) presented a model relating the exponent of the power law to the potential of the electron in QDs in the matrix and traps. The reason for most of the observed exponents in QDs to be close to $-3/2$ remained to be explored for this model. Flomenbom et al. (53) investigated two-state single-molecule trajectories arisen from a multi-substrate kinetics. In the work of Boguna et al. (47), a stochastic two-state model was presented to obtain the relationship between the lifetime distribution function for intermittency and the ensemble intensity. Such a model was later applied by Margolin and Barkai (49) where they considered either a power law or an exponential decay for the lifetime distribution. These relations could be derived using the DCET model as well, which provides a molecular basis for the kinetic parameters and the stochastic nature of energy fluctuations.

Tang and Marcus proposed a diffusion-controlled electron transfer mechanism (20, 50) to elucidate the inverse power-law blinking statistics of single QDs and quasi-stretched exponential decay (51) of fluorescence intensity decay $\langle I(t)\rangle$ of an ensemble of QDs. This model offers the explanations to these time profiles and the relationship between the fluorescence intensity for an ensemble of QDs, $\langle I(t)\rangle$, and the waiting time distribution $P(t)$ for both light and dark events in single QDs.

Modeling photoluminescence of single nanoparticles

Photoluminescence of semiconducting nanocrystals has been investigated on a single particle level as well as in an ensemble system. The fluorescence intensity histogram of a single QD under continuous light illumination usually displays bi-level blinking or a more complicated pattern. The distribution of the on- or off-time events, or often called blinking statistics, exhibits an inverse power law. For the on-events, deviations from the simple power-law behavior with an exponential or stretched exponential tail are often seen at a longer time. The extension of the bending for such a bending tail also appears to depend on the size of the nanoparticles, the excitation intensity, and the temperature. However, for the off-events, the bending tail would appear at a much later time and does not seem to depend on the particle sizes and the excitation intensity. These sorts of behaviors could be explained by the DCET model of Tang and Marcus based on the diffusion-controlled electron transfer model with diffusion in one-dimensional (1-D) energy space (20, 50). The cause for the stretched exponential decay observed experimentally in nanorods (NRs) was explained through a generalized DCET model by including anomalous diffusion in the work of Tang and Marcus (20). Here, we discuss the model for fluorescence intermittency of single nanoparticles and time profile of fluorescence intensity for an ensemble of nanoparticles. The relationship between the inverse power law of single nanoparticles and the quasi-stretched exponential time profile of an ensemble system was elucidated in the work of Tang and Marcus. We will first describe the DCET model involving anomalous diffusion. The DCET model with normal diffusion predicted the exponent of an inverse power law to be 1.5. As a special case, the exponent of the long-time exponential decay would not be 1.5 with a long-time stretched exponential bending tail. In the section that follows we will discuss the model for the fluorescence intensity time profile for an ensemble of QDs, which succeed quasi-stretched exponential decay.

Diffusion-controlled electron transfer (DCET) model involving anomalous diffusion

In the DCET model for power-law blinking behavior of single QDs, we considered electron transfer between a pair of states: a light state and a dark state as illustrated by Fig. 1. The light state represents the photoexcited state of a single QD with an exciton. The electron and the hole of this neutral excitonic state could recombine radiatively by emitting a fluorescence photon. Thus, the population of the light state returns frequently to the ground state by photoemission. In addition, the light state could be

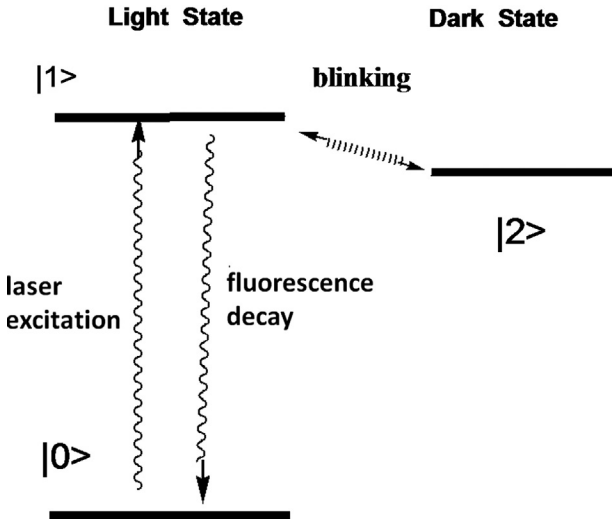

Fig. 1. A schematic energy diagram for relevant states for blinking of a QD, showing the light state $|1>$, the dark state $|2>$, and the ground state $|0>$.

populated by photoexcitation from the ground state upon continuous light illumination. The dark state represents a charge-separated state with a mobile hole residing in the core of a QD (or NR) and an electron trapped on surface states due to the surface defects. This dark state occurred because the mobile hole acts as a fast energy relaxation agent, which absorbs the excessive and non-radiative energy from further excitonic photoexcitation through Auger process. Charge transfer or recombination could occur between the neutral light state and the charge-separated dark state. The electron transfer (ET) rate between these two states under continuous light illumination is not constant. Due to stochastic variations in the energetic configuration space or the distance between the hole and the electron, the rate is always subject to fluctuations. The energy fluctuations could be modeled as a central oscillator in the presence of interactions with oscillators in the heat bath, and the probability distribution function $\rho(Q, t)$ is given by

$$\rho(Q,t)=\frac{1}{\sqrt{2\pi\Delta_2(t)}}\exp\left[-\frac{\left(Q-\langle Q(t)\rangle\right)^2}{2\Delta_2(t)}\right]. \tag{1}$$

This Gaussian probability distribution function $\rho(Q, t)$ could be used to satisfy the following time-dependent diffusion equation in a parabolic potential

$$\frac{\partial}{\partial t}\rho(Q,t)=\frac{\partial}{\partial Q}\left(D_2(t)\frac{\partial}{\partial Q}+D_1(t)Q\right)\rho(Q,t), \tag{2a}$$

where

$$D_1(t)=-\frac{d}{dt}\ln\langle Q(t)\rangle$$

$$D_2(t)=D_1(t)\Delta_2(t)+\frac{1}{2}\frac{d}{dt}\Delta_2(t). \tag{2b}$$

If the diffusion coefficient D_1 and the drift coefficient D_2 are constant in time, which is the case for normal diffusion in Debye dielectric medium; then, in a harmonic potential if $D_2 = D$ and $D_1 = 1/\tau_c$, where τ_c is the diffusion correlation time constant, Equation 2 becomes the well-known 1-D diffusion equation.

In the DCET model (20), a 1-D diffusion equation involving a Dirac δ-function population sink was considered. As illustrated in Fig. 2, population exchange occurs between light and dark states at the energy level crossing between two parabolic potentials. In a more refined model, such a figure could be reduced from the 2-D diffusion-controlled reaction (DCR) model (54) involving both the fast reaction coordinate q and slow reaction coordinate Q where the fluctuations in activation energy occurs at a much slower time scale, whereas the electron transfer can proceed very fast.

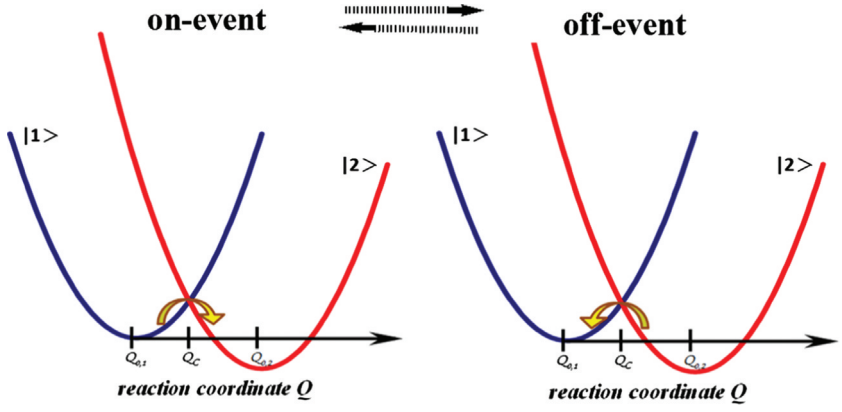

Fig. 2. Intermittency as controlled by 1-D diffusion in energy space via a sink at the energy-level crossing of two parabolic potential wells of a light $|1>$ state and a dark state $|2>$.

Citation: Nano Reviews 2011, **2**: 5895 - DOI: 10.3402/nano.v2i0.5895

As explained in our previous work (50, 55), due to fast diffusion along q on two Marcus's parabola, such a 2-D coupled rate equation could be reduced to 1-D diffusion along Q on a harmonic potential with a Gaussian-shaped sink, instead of a Dirac δ-function sink. The governing equation for the probability $\rho(Q, t)$ for either forward or reverse ET is given by

$$\frac{\partial}{\partial t}\rho(Q,t) = \frac{\partial}{\partial Q}\left(D_2(t)\frac{\partial}{\partial Q} + D_1(t)Q\right)\rho(Q,t) - k(Q)\rho(Q,t), \tag{3a}$$

where the fluctuating ET rate $k(Q)$ is given by

$$k(Q) = \frac{A}{\sqrt{2\pi}\sigma}\exp(-(Q-Q_0)^2/2\sigma^2)\rho(Q,t),\ A \equiv \frac{2\pi|V_{ex}|^2}{\hbar}\frac{1}{\sqrt{4\pi\lambda k_B T}}, \tag{3b}$$

where V_{ex} is the electronic coupling strength. The last term in Equation 3a describes depopulation via a sink with a fluctuating transition rate $k(Q)$ depending on the slow reaction coordinate Q. After the reduction of the fast diffusion in the 2-D diffusion model, one could obtain 1-D diffusion in a parabolic potential of the slow reaction coordinate Q with a sink around Q_0. If the second moment σ^2 is small and $k(Q)$ can be approximated by $\delta(Q-Q_0)$ Such a Dirac δ-function sink was assumed in our previous DCET model (20). The fluctuating sink rate $k(Q)$ is modulated by a stochastic variable Q. Such fluctuations can be caused either by changes in the barrier height due to conformation variations or changes in the distance between the electron-hole pair via the electronic coupling element. The energy fluctuations of the surface trap states of a nanoparticle might be the primary cause, instead of electron-donor distance fluctuations caused by physical hopping of the charge on the surface.

Using the Green's function method, we solved Equation 3 to obtain $\overline{\rho}(Q,s)$, the Laplace transform of the population $\rho(Q,t)$, as

$$\overline{\rho}(Q,s) = \frac{\overline{G}(Q,Q_0;s)}{1 + A\overline{G}(Q_0,Q_0;s)}. \tag{4}$$

The Laplace transform of the blinking statistics $P(t)$, which is defined as the waiting-time distribution of the 'on' or 'off' events, is given by

$$\overline{P}(s) = -\int_0^\infty dt e^{-st}\frac{d}{dt}\left(\int_{-\infty}^{\infty} dQ\rho(Q,t)\right) = \frac{A\overline{G}(Q_0,Q_0;s)}{1 + A\overline{G}(Q_0,Q_0;s)}. \tag{5a}$$

The Laplace transform of the Green function for Equation 2 of a sink-free diffusion is given by

$$\bar{G}(Q_0,Q_0;s) = \int_0^\infty dt e^{-st}\frac{1}{\sqrt{2\pi\Delta_2(t)}} \exp\left[-\frac{Q_0^2(1-\Delta_1(t)^2}{2\Delta_2(t)}\right]. \tag{5b}$$

Here the simple normal diffusion case would be considered first. At a short time $t << \tau_c$ with

$$\Delta_2(t) = D\tau_c(1-\exp(-2t/\tau_c)) \approx 2Dt$$

and

$$1-\Delta_1(t) = 1-\exp(-t/\tau_c) \approx t/\tau_c,$$

one obtains

$$\overline{G}(Q_0,Q_0;s) \approx \frac{1}{\sqrt{4\pi D(s+\Gamma)}}. \tag{6}$$

By inverse Laplace transform of Equation 5a using the above $\overline{G}(Q_0,Q_0;s)$ one could obtain

$$P(t) \propto t^{-3/2}\exp(-\Gamma t),\quad \Gamma = Q_0^2/4D\tau_c^2 = \kappa Q_0^2/4k_BT\tau_c \equiv E_A/2k_BT\tau_c, \tag{7}$$

where $E_A \equiv \kappa Q_0^2/2$ is the activation energy. Equation 7 shows a power-law statistic with an exponent $-3/2$ as expected from the usual first passage theory. In addition, Equation 7 also displays a crossover to an exponential bending tail with a bending rate Γ. The above temporal behavior for $P(t)$ derived in the regime of short time $t << \tau_c$ is primarily due to slow diffusion that modulates the ET rate, $k(Q)$. If the diffusion is fast with a very short τ_c, the blinking statistics would become an usual exponential decay (20, 51) instead of an inverse power law. Such behavior with an exponential decay is expected from the conventional electron transfer theory that is equivalent to the diffusion-controlled reaction with a very fast spectral diffusion. In Fig. 3, we use the data of CdTe QDs at 300 K and 125 W/cm2 (taken from Shimizu et al. (25)) as an example to illustrate the inverse power-law behavior and the fit using Equation 7.

Now we describe the more complicated anomalous diffusion case. Here we consider a non-Debye medium with Kohlrausch-Williams-Watts (KWW) function (56) as

$$\Delta_2(t) = \Delta_2(\infty)[1-\exp(-(t/\tau_c)^\mu)] \approx \Delta_2(\infty)(t/\tau_c)^\mu \tag{8a}$$

and

$$1-\Delta_1(t) = 1-\exp(-(t/\tau_c)^\nu) \approx (t/\tau_c)^\nu. \tag{8b}$$

As shown in our previous work 57) that with a coupled central oscillator to heat bath, one could explain how the spectral distribution of bath modes can give rise to such KWW behavior for Δ_2(t) and Δ_1(t). The Green function of Equation 5b for such Δ_2(t) and Δ_1(t) can be approximated by

$$\overline{G}(Q_0,Q_0;s) \approx \int_0^\infty dt e^{-st}\frac{(t/\tau_c)^{-\mu/2}}{\sqrt{2\pi\Delta_2(\infty)}}$$

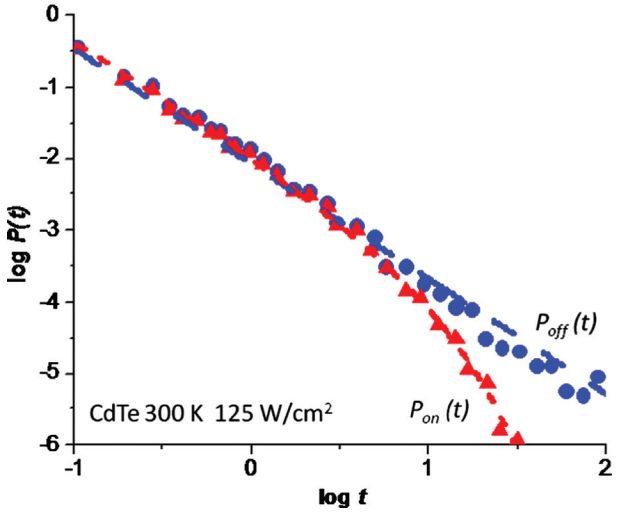

Fig. 3. The log-log plot of the blinking statistics $P(t)$ versus time t for data of both 'off' and 'on' events of CdTe QDs at 300 K and 125 W/cm^2 with the fit using Equation 7 (taken from Shimizu et al. (25)).

$$\exp\left[-\frac{Q_0^2}{2\Delta_2(\infty)}(t/\tau_c)^{2\nu-\mu}\right]. \tag{9}$$

Using the Green function in Equation 9, one could evaluate the blinking statistics $P(t)$ from Equation 5a using numerical inverse Laplace transform.

An exact analytic inverse Laplace transform of Equation 5a for the Green function of Equation 9 is not available. In order to observe a stretched exponential tail arising for the blinking statistics, one can use the following approach with Taylor series expansion. One obtains from Equation 5 the integrated population as

$$\begin{aligned}\overline{\rho}(s) &= \int_{-\infty}^{\infty} dQ \frac{\overline{G}(Q, Q_0; s)}{1 + A\overline{G}(Q_0, Q_0; s)} \\ &= \frac{1}{s}\cdot\frac{1}{1 + A\overline{G}(Q_0, Q_0; s)}.\end{aligned} \tag{10}$$

In the regime with strong sink strength A, one has

$$\begin{aligned}\overline{\rho}(s) \approx \frac{\sqrt{2\pi\Delta_2(\infty)}}{A}\Bigg[&\frac{(\tau_c s)^{-\mu/2}}{\Gamma\left(1-\frac{\mu}{2}\right)} \\ &+\frac{Q_0^2\Gamma\left(2\nu+1-\frac{3\mu}{2}\right)(\tau_c s)^{-2\nu+\mu/2}}{2\Delta_2(\infty)\Gamma\left(1-\frac{\mu}{2}\right)}+\cdots\Bigg]\end{aligned} \tag{11}$$

Using the inverse Laplace transform of Equation 11 in time domain, we obtain the blinking statistics $P(t)$ as

$$\begin{aligned}P(t) \equiv -\frac{d}{dt}\rho(t) &\approx P_0(t/\tau_c)^{-2+\mu/2}\exp(-(\Gamma t)^{2\nu-\mu}) \\ &\propto t^{-m}\exp(-(\Gamma t)^n).\end{aligned} \tag{12}$$

Equation 12 shows an inverse power law with an exponent $m = 2-\mu/2$, and an exponent n for the stretched exponential with $n = 2\nu-\mu$. Equation 12 has been used in our recent work of CdSe nanorods (58, 59). Here we present the derivation and its relationship to anomalous diffusion and the quantum Brownian motion of a central oscillator. The more general formula in Equation 12 for anomalous diffusion reduces to Equation 7 of normal diffusion if $\mu = \nu = 1$.

In the limit of a weak sink strength A with a small A, using the similar procedure given above, we obtain

$$\begin{aligned}&P(t) \propto (t/\tau_c)^{-\mu/2} \\ &\exp[-(\Gamma t)^{2\nu-\mu}] \propto t^{-m}\exp[-(\Gamma t)^n],\end{aligned} \tag{13}$$

showing an inverse power law with an exponent $m = \mu/2$ and a stretched exponential tail with an exponent $n = 2\nu-\mu$. According to this model, the exponent m of the short-time power law for a weak A as obtained in Equation 13 is different from the exponent in Equation 12 for a strong A. However, their sum equals to 2 exactly. The inverse power-law blinking statistics for these two regimes for either the normal or anomalous diffusion case is shown in Fig. 4.

To compare the theoretical predictions for the anomalous diffusion case with experimental results, we consider some examples here. The experimental and fitted curves of $P_{on}(t)$ and $P_{off}(t)$ for samples NR5 and NR7 are illustrated in Fig. 5a. The exponents for the power law of $P_{on}(t)$ and $P_{off}(t)$ appear to be slightly different with $m_{on} = 1.35$ ($\pm$ 0.05) and $m_{off} = 1.10$ ($\pm$ 0.05). The long-time tail for $P_{on}(t)$ yields $n_{on} = 0.85 \pm 0.05$. The long-time tail of $P_{off}(t)$ for the 'off' events, however, is highly non-exponential and it can only be described best by a stretched exponential of $n_{off} = 0.30 \pm 0.05$. In Fig. 5b, the

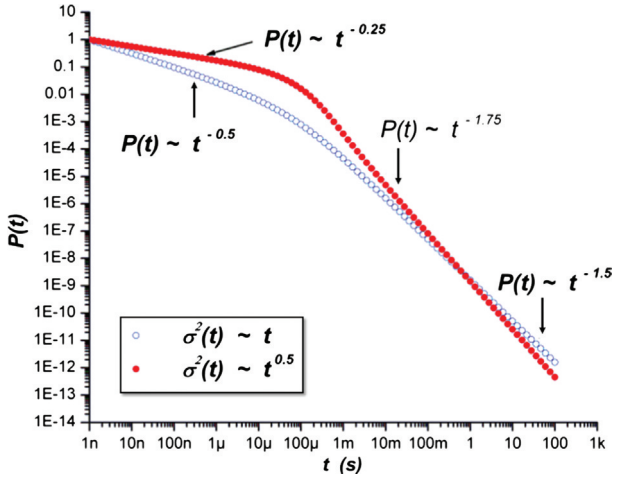

Fig. 4. Blinking statistics $P(t)$ for DCET model with normal diffusion ($\beta_{CD} = 1$) and anomalous diffusion ($\beta_{CD} \neq 1$). The exponent for the power law depends on β_{CD} of the dielectric medium. At a much shorter time than t_c (set arbitrarily at 10^{-4} s), $P(t)$ follows a different power law.

Citation: Nano Reviews 2011, **2**: 5895 - DOI: 10.3402/nano.v2i0.5895

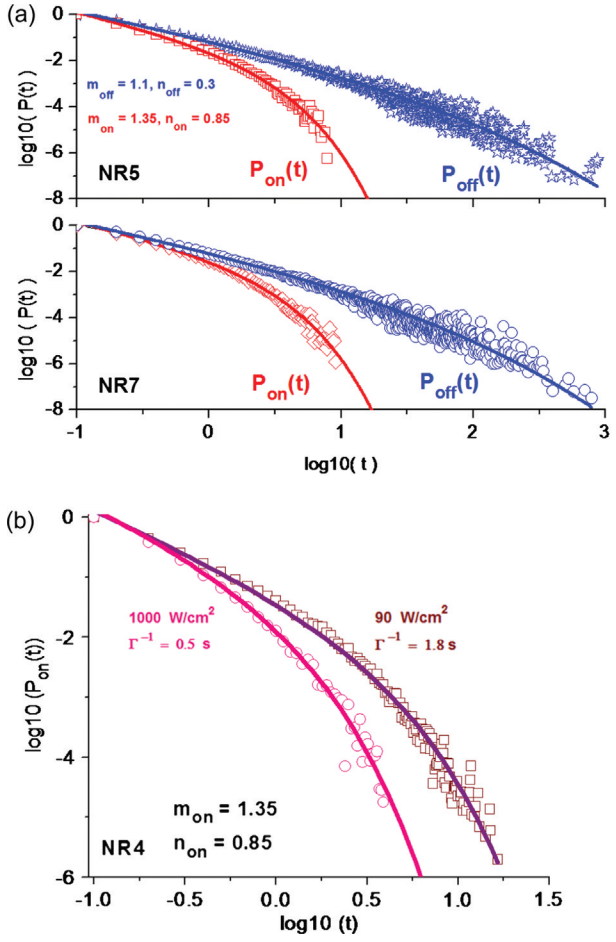

Fig. 5. (a) The blinking statistics $P(t)$ of the 'on' and 'off' events for samples NR5 (top) and NR7 (bottom) in a log-log plot with fitted solid curves. The bending tail for $P_{off}(t)$ is not single exponential and can be best fitted using $t^{-m}\exp[-(\Gamma t)^n]$. (b) Log-log plot of $P_{on}(t)$ and the fitted curve for sample NR4 at two light intensities, showing a greater bending rate at a higher intensity. The time unit is in seconds.

fit and the experimental data of $P_{on}(t)$ for NR4 at two different excitation intensities are demonstrated. Anomalous diffusion occurs in a disordered system with dispersive diffusion correlation times (13). The presence of strong anomalous diffusion for NRs or QDs in the dark state might have been due to the existence of many possible surface trap states for the electron in the charge-separated state. These trap states could have different energies and lead to spectral diffusion in the energy configuration space. More details about the data fitting will be given in the following section.

Modeling ensemble-averaged fluorescence intensity time profile

As discussed earlier, in the treatment of single-particle blinking statistics each particle is distinguishable. Therefore, the rate equations for the forward and inverse ET should be decoupled. However, in ensemble measurements, nanoparticles are indistinguishable and there is no prior information about whether a nanoparticle is in light or dark state. To treat ensemble-averaged fluorescence intensity, one has to use the coupled rate equation with both forward and reverse ET process. In single-QD intermittency studies, above, only the short time power-law behavior was the major interest. To calculate longer time behavior for single QD or the ensemble fluorescence intensity over the entire time span, one needs to solve the coupled rate equation given by

$$\frac{\partial}{\partial t}\rho_1(Q,t) = \int_0^t d\tau L_1(t-\tau)\rho_1(Q,\tau) - \frac{2\pi|V_k|^2}{\hbar}\delta(U_{12}(Q))$$
$$(\rho_1(Q,t) - \rho_2(Q,t))$$
$$\frac{\partial}{\partial t}\rho_2(Q,t) = \int_0^t d\tau L_2(t-\tau)\rho_2(Q,\tau) - \frac{2\pi|V_k|^2}{\hbar}\delta(U_{12}(Q))$$
$$(\rho_2(Q,t) - \rho_1(Q,t)), \qquad (14)$$

where

$$L_k(\tau) \equiv \Delta_k^2\varphi_k(\tau)\frac{\partial}{\partial Q}\left(\frac{\partial}{\partial Q} + \frac{\partial}{\partial Q}(U_k(Q)/k_BT)\right),$$
$$\text{and } \overline{\varphi_k}(s) = (s\tau_{D,k}+1)^{1-\beta_{CD}}/\tau_{L,k}.$$

Equation 14 becomes Markovian if $\beta_{CD}=1$ where $\varphi_k(t)=\delta(t)/\tau_{L,k}$. Defining $\bar{G}_k(Q,Q';s)$, the Green function in the Laplace transform domain, that satisfies $s\overline{G}_k(Q,Q';s) - \overline{L}_k(s)\overline{G}_k(Q,Q';s) = \delta(Q-Q')$, one obtains from Equation 14

$$\langle\overline{\rho}_1(s)\rangle = \frac{1}{s}\int_{-\infty}^{\infty} dQ\rho_1(Q,0)$$
$$- \frac{\int_{-\infty}^{\infty} dQA_1\overline{G}_1(Q_c,Q;s)\rho_1(Q,0) - \int_{-\infty}^{\infty} dQA_2\overline{G}_2(Q_c,Q;s)\rho_2(Q,0)}{s(1 + A_1\overline{G}_1(Q_c,Q_c;s) + A_2\overline{G}_2(Q_c,Q_c;s))}. \qquad (15)$$

As illustrated in Fig. 6, the initial population of QDs on the left parabola representing the light state will evolve in time and will eventually reach equilibrium at longer times. If a QD ensemble is initially in the light state

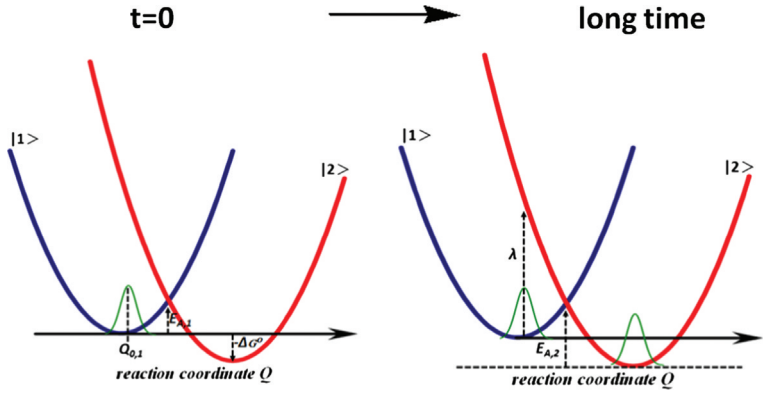

Fig. 6. Time evolution of an initial Gaussian population distribution in $|1>$ centered at $Q_{0,1}$. At longer times a steady-state distribution is established between $|1>$ and $|2>$. The relation of forward/reverse ET activation energy ($E_{A,1}/E_{A,2}$), reorganization energy (λ) and free energy gap (ΔG^0) to two parabolas are illustrated.

$|1>$ with a Boltzmann distribution, $\rho_1(Q,0) = (1/\sqrt{2\pi k_B T/\kappa})\exp(-\kappa(Q-Q_{0,1})^2/2k_B T)$, the normalized intensity $\langle \overline{I}(s)\rangle$ can be derived from Equation 15 (52)

$$\langle \overline{I}(s)\rangle = \langle \overline{\rho}_1(s)\rangle = \frac{1}{s}\left[1 - \frac{\gamma_1}{s(1+\overline{g}_1(s)+\overline{g}_2(s))}\right], \tag{16}$$

where γ_1 and γ_2 are the non-adiabatic forward and reverse reaction rates. Defining the relaxation function $\langle \overline{R}(s)\rangle$ as $\langle \overline{R}(s)\rangle(1-I_{eq}) \equiv \langle \overline{I}(s)\rangle - I_{eq}/s$ from Equation 16 one has

$$\langle \overline{R}(s)\rangle = \frac{1}{s}\left[1 - \frac{\gamma_1+\gamma_2}{s(1+\overline{g}_1(s)+\overline{g}_2(s))}\right]. \tag{17}$$

The steady-state intensity is given by (51)

$$I_{eq} = \frac{1}{1+\varsigma_1 \exp(-\Delta G^0/k_B T)}. \tag{18}$$

One can also express Equation 17 as (51)

$$\langle \overline{I}(s)\rangle = \frac{1}{s}\left[1 - \frac{\gamma_1(1-\overline{P}_1(s))(1-\overline{P}_2(s))}{s(1-\overline{P}_1(s)\overline{P}_2(s))}\right] \tag{19}$$

and Equation (17) as (51)

$$\langle \overline{R}(s)\rangle = \frac{1}{s}\left[1 - \frac{\gamma_1+\gamma_2}{s}\frac{(1-\overline{P}_1(s))(1-\overline{P}_2(s))}{1-\overline{P}_1(s)\overline{P}_2(s)}\right]. \tag{20}$$

Equations 16–20 represent the relationship between ensemble-averaged behavior and blinking statistics $\overline{P}_k(s)$ of single QDs.

Equations 16–20 have been derived previously by Boguna et al. (47), and they were applied by others including Brokmann et al. (33), Verberk et al. (34), Verberk and Orrit (35), and Margolin and Barkai (49) to characterize asymptotic behavior of QDs. Equation 20 only applies when an initial population is at the energy level crossing, and it was used previously by Bardou and Bouchaud (60) for laser cooling. It was recently applied by Chung and Bawendi (27) to ensemble studies. These equations were previously expressed in terms of $\overline{P}_k(s)$ and $\langle \tau_k\rangle$). Here, we showed $\langle \tau_k\rangle^{-1} = {}_k$, which is simply the non-adiabatic electron transfer rate. More importantly, via $\overline{g}_k(s)$, Equations 16–20 provide formulas calculable for the entire time span (for anomalous/normal diffusion model), while linking $\langle I(t)\rangle$ and $P_k(t)$ to measurable molecular-based quantities.

Some calculated curves based on Equation 16 with a Debye medium are illustrated in Fig. 7, showing a fit to a stretched exponential $I_{eq} + (1-I_{eq})\exp(-(t/T_0)^{\alpha})$. At much longer times, they decay exponentially. As an example for the applications of the equations derived in this section for ensemble-averaged behavior, fluorescence intensity decay data of CdSe with a ZnS shell are compared with Equation 16 as illustrated in Fig. 8. From the fits, we estimated some molecular-based kinetic and energetic parameters.

The $\langle \overline{I}(s)\rangle$of Equation 19 is related to the auto-correlation of fluorescence intensity of others by

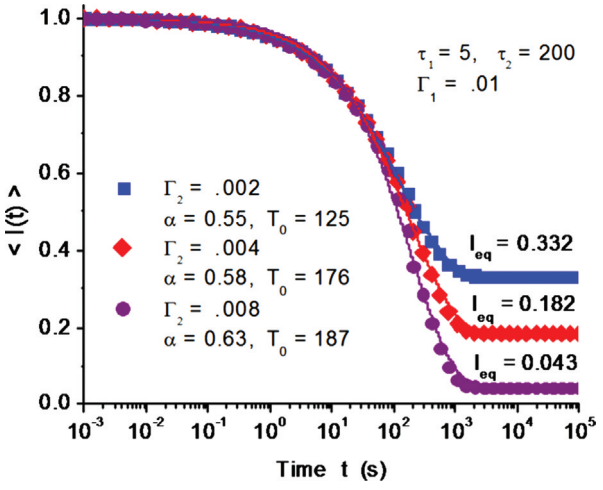

Fig. 7. Semi-log plot of fluorescence intensity profile $\langle I(t)\rangle$ (dot curves) for a QD ensemble and the fitted (solid) curves by a stretched exponential $I_{eq} + (1-I_{eq})exp(-(t/T_0)^{\alpha})$ with fitted values for α and T_0 $\beta_{CD} = 1$ was used.

Citation: Nano Reviews 2011, **2**: 5895 - DOI: 10.3402/nano.v2i0.5895

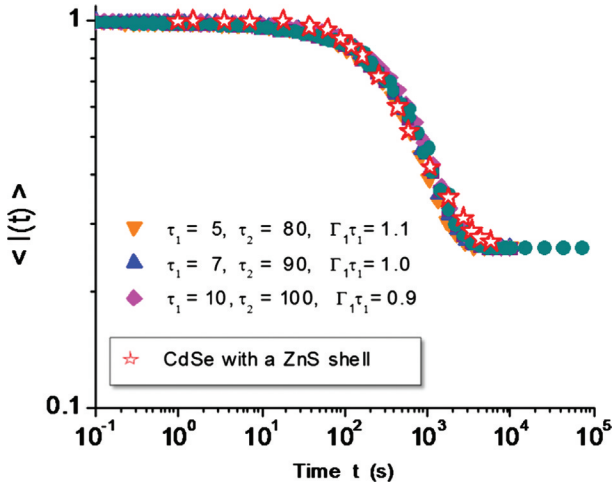

Fig. 8. Log-log plot of experimental $\langle I(t)\rangle$ (dot curves) and the fitted (solid) curves using Equation 18. From $I_{eq} \sim 0.26$ at the long times, we estimated $\Delta G^0 \sim -33$ meV. Using $\zeta_1 \sim 0.75$, $\tau_1 \sim 10$ s, and $\tau_2 \sim 100$ s, we estimated $E_{A,1} \sim 57$ and $E_{A,2} \sim 52$ meV (adapted from reference36).

$\langle I(s)\rangle = \overline{C}_F(s)\gamma_2/(\gamma_1+\gamma_2)$. As illustrated by the experimental data of CdSe QDs by Messin et al. (33) with a very large time constant for a correlator, $C_F(t)/C_F(0)$, behaves as $\langle I(t)\rangle$ (or $\langle R(t)\rangle$ at short time). Unusual time dependence in $\langle I(t)\rangle$ and $\langle R(t)\rangle$arises if P_{on} (t) and $P_{off}(t)$ follow different decaying laws. Such a situation has been extensively studied by Margolin and Barkai (49) using a phenomenological $P_k(t)$. It can be analyzed in this study by assigning a different β_{CD} for $\overline{g}_k(s)$ for the light and dark states. As an example, if $P_{off}(t)$ follows a power law while $P_{on}(t)$ decays single exponentially as $\gamma_1 \exp(-\gamma_1 t)$, we obtain $C_F(t) \sim (t/t_{c,2})^{-\beta_{CD,2}/2}(\gamma_1+\gamma_2)/\Gamma(1-\beta_{CD,2}/2)\gamma_1\gamma_2 t_{c,2}$.

Control of fluorescence intermittency and electron transfer

Fluorescence blinking is a very interesting phenomenon, yet it is a serious drawback for practical applications in quantum optics and single-molecule spectroscopy. Therefore, suppression of fluorescence blinking is an important issue in this research field. Here, we will mainly focus on recent progress on blinking suppression via various strategies including physical, chemical, and material science methods. In addition, we will discuss the phenomena by using the diffusion-controlled electron transfer (DCET) model of Tang and Marcus.

Blinking suppression by encapsulating single QDs in agarose gel

To investigate how the environment affects fluorescence blinking of single QDs, we encapsulate single QDs in agarose gel (61). Fig. 9 shows the fluorescence intensity trajectories of single CdSe/ZnS QDs on a glass substrate, in 0.3% and in 1% agarose gel by binning the detected photons within a 1 ms window. The stochastic fluctuation between fluorescent 'on' level and dark 'off' level was observed for single QDs on glass and QDs embedded in 0.3% gel. The photon count distribution of two distinguishing intensity levels related to the 'on' and 'off' states is displayed on the right of the intensity trajectory. Compared with QDs on glass and in 0.3% agarose gel,

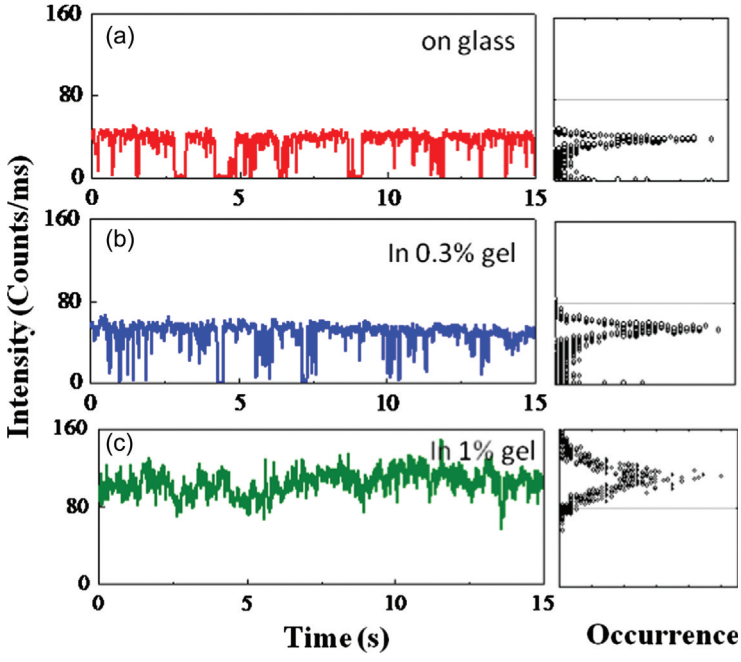

Fig. 9. (a) Fluorescence intensity trajectory and its corresponding photon count histogram from single CdSe/ZnS QDs spin-coated on a glass substrate,. (b) for spin-coated single QDs in 0.3% gel, (c) for spin-coated single QDs in 1% gel.

the time trace for single QDs in 1% gel exhibits essentially continuous emission without dark periods (Fig. 9c). The SEM images of agarose gel with the concentrations of 0.3% and 1% are shown in Fig. 10 to illustrate the influence of the concentration on the pore size. The pore diameters of the 1% gel structure were found to be ~200 nm and the pore diameters were around 8 μm for 0.3% gel. This result agrees with the previous work where the pore diameter increases as the agarose concentration decreases and the pore diameter distribution narrows as the gel concentration increases (62). Agarose gel fibers were found to be inherently negatively charged, due to the sufficient amount of charged groups such as pyruvate, sulfate, and methoxy groups in commercially prepared agarose (63–65). Generally speaking, if the electron transitions from the light state to the dark state could be blocked, then blinking would be suppressed. In addition, the negative charges on the pore surface could reduce the tunneling rate of the electron to the surface. Therefore, we suggest that the negative charges on agarose gel fibers could play an important role in this blinking suppression behavior.

Fig. 11a presents the decay profiles of single QDs on a glass substrate and in 1% agarose gel. The average fluorescence lifetime of QDs embedded in 1% agarose gel is about 19 ns, which is faster than that of QDs on glass (28 ns). The negative charges inherent with gel fibers could influence the blinking and the fluorescence decay.

We also observed that an increase of gel concentration could enhance the fluorescence quantum yield. Fig. 11b shows the relationship between gel concentration and total photon counts from the fluorescence time traces by summing up over 20 QDs, where the light intensity was set at 0.67 KW/cm^2. The photon counts were found to be linearly related to the gel concentration. In general, the quantum yield of a natural emitter could be given by $Q = \gamma/(\gamma + k_{nr}) = \gamma \times \tau$, where γ, k_{nr} and τ are the radiative, non-radiative, and measured fluorescence lifetimes, respectively. Therefore, we estimated nearly 3.8-fold increase in the radiative rate, as compared between QDs on glass and embedded in 1% agarose gel.

To clarify that the observed non-blinking behavior in agarose gel is not due to aggregation of QDs, photon correlation measurements were performed. This inference agrees with the results of photon correlation measurements. Second-order intensity autocorrelation function, g^2 (τ), for single QDs embedded in 1% agarose gel is shown in Fig. 12. The data were binned with 400 ps time intervals and acquired for ~30 min. The g^2 (τ) function can be approximated as $g^2(\tau) \cong 1 - 1/N \exp[-\tau(W_P + \Gamma_{fl})]$, where N, W_p, and Γ_{fl} are the number of independent emitters, excitation rates, and fluorescence recombination rates, respectively. It is well known that the value of $g(2)$ (τ) equals to 0.5 for two independent emitters. In our case the value of g^2 (τ) is around 0.23, which is still less than 0.5. The residual g^2 (τ) value could be attributed to

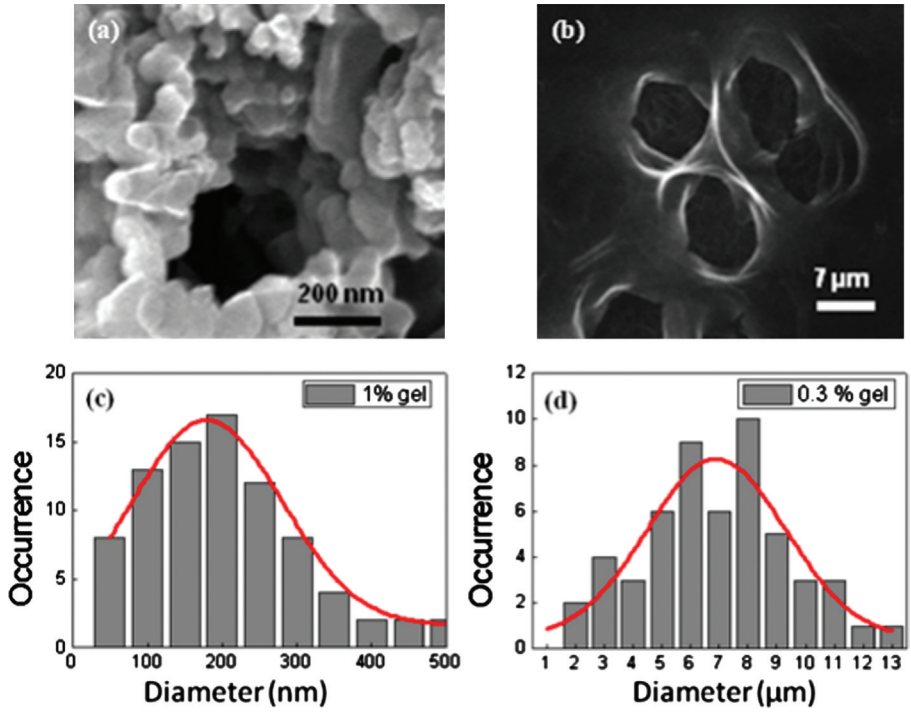

Fig. 10. (a) SEM cross-sectional view of 1% agarose gel at 50000 ×. (b) SEM cross-sectional view of the 0.3% agarose gel at 1600 ×. (c) Pore diameter distribution for 1% gel obtained from the SEM images. The peak distribution of the pore diameters is around 200 nm. (d) Pore diameter distribution for 0.3% gel obtained from the SEM images. The peak distribution of the pore diameters is around 8 μm.

Citation: Nano Reviews 2011, **2**: 5895 - DOI: 10.3402/nano.v2i0.5895

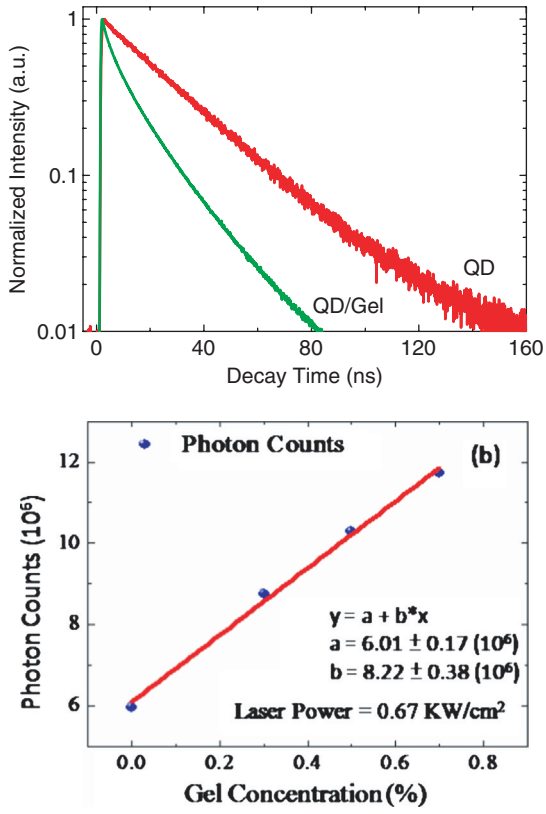

Fig. 11. (a) Fluorescence decay profiles for single QDs on a glass substrate and embedded in 1% agarose gel. (b) The relationship between gel concentration and the total photon counts for the fluorescence time traces by summing up over 20 QDs.

agarose gel that yields a low fluorescence background. Therefore, this photon anti-bunching behavior is the hallmark for single photon emission from an individual QD rather than emission from aggregated QDs.

Fig. 13 shows the on-time distribution $P_{on}(t)$ of single QDs on glass, in 0.3, 0.5, and 0.7% gel. An inverse power-law distribution was demonstrated at shorter times but then deviated from this distribution at longer times, exhibiting an exponential bending tail. The distribution was fitted using $P(t) \sim ct^{-m}$ exp($-\Gamma t$), where c is an unimportant scaling constant, m is the power-law exponent, and Γ is the bending rate. In our cases, m is typically around 1.0–1.5. Compared with QDs on glass, the bending rate Γ becomes greater as the gel concentration increases, which is illustrated in Fig. 14. The details of such findings were presented in our recent report (61).

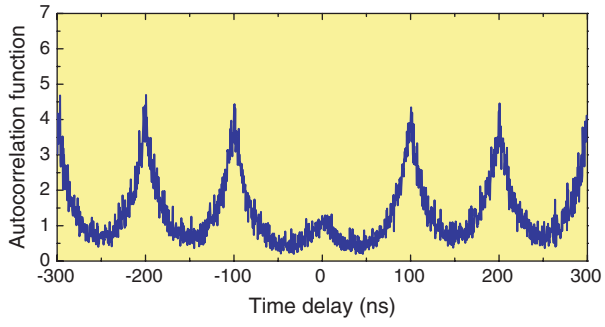

Fig. 12. Photon correlation measurements of QDs embedded in 1% agarose gel, exhibiting anti-bunching behavior.

According to the diffusion-controlled electron transfer (DCET) model of Tang and Marcus (20, 50) and Tang (57), Γ increases with the activation energy for electron transfer from the light state to the dark state. Therefore, our data demonstrates that the activation energy also increases with the gel concentration. The activation energy might become too large at a much higher concentration for charge transfer or blinking to occur. We suggest that the negative charges surrounding the quantum dots might play an important role in controlling charge transfer and blinking suppression. Unlike the on-events, the occurrence of the off-events is less frequent for QDs in gel, and it becomes completely absent for the case with 1% gel. Therefore, the noise level of the waiting time distribution during the dark events would be too high for a meaningful analysis.

The schematic of the DCET model is illustrated in Fig. 15 (20, 50, 51, 57). In general, the power-law exponent, m, for 'on' and 'off' times equals to 1.5 exactly for normal diffusion but deviation occurs for anomalous diffusion. However, the exponential bending rate Γ is related to the activation energy for the electron transfer process from the light state $|L^*>$ to the dark state $|D>$. We suggest that the negative charges form gel fibers surrounding the QDs could cause an energy up-shift of $|D>$ with respect to $|L^*>$ and it would result in an increased activation energy. Therefore, the transition rate from the neutral light state to the charged dark state could be reduced.

Influence of blinking by conductive substrate on spin-coated QDs

In the following section, we will discuss the recent studies of single QDs on conductive substrates to explore the environmental effects on photoluminescence properties of QDs. When single colloidal QDs were placed near noble metal substrates such as Au and Ag, there are complex interactions between them including plasmonic interactions, energy and charge transfer processes. Therefore, the blinking behavior can be modified dramatically (66–69). As an example, blinking behavior of single colloidal QDs could be suppressed by depositing them onto silver nanoprisms directly (66). Other conductive substrates, such as ITO substrate as an example, are also important and interesting materials to demonstrate their influence on the single-QD blinking behavior (70). Usually, we observed two types of fluorescence time trajectories for single colloidal CdSe/ZnS QDs on ITO substrates as shown in Fig. 16a and b. For the first type, the behavior is similar

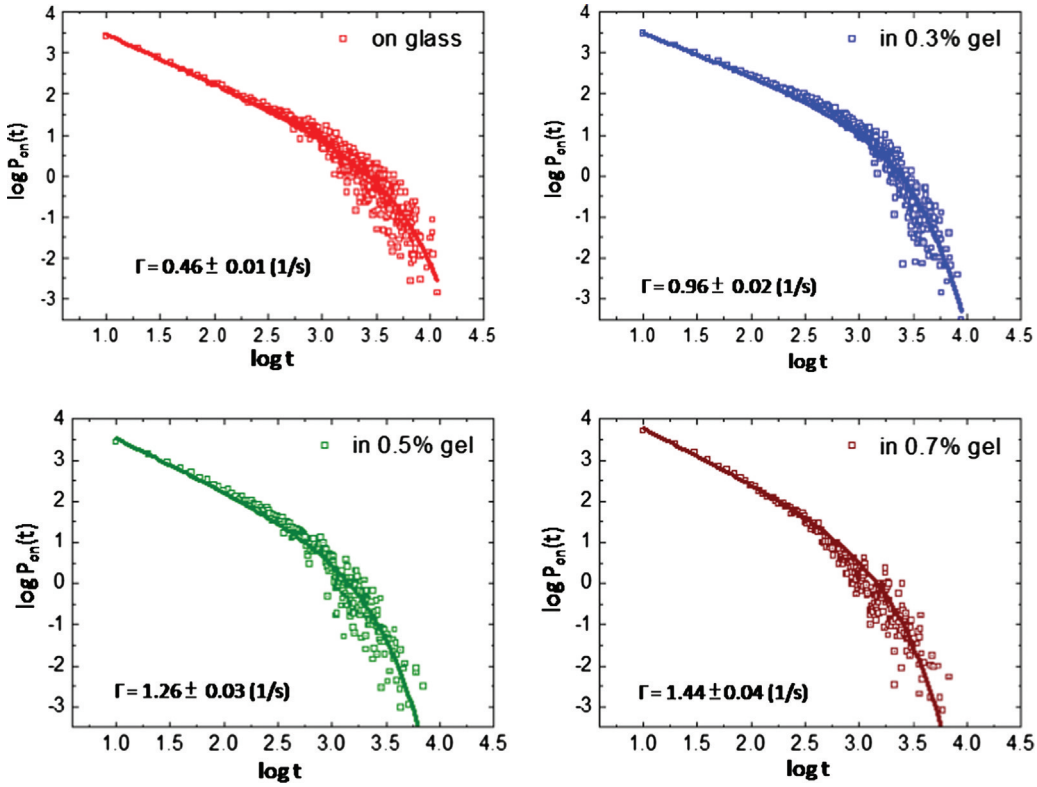

Fig. 13. On-time blinking statistics of single QDs on glass in 0.3%, 0.5%, and 0.7% gel, respectively.

to the conventional QDs with typical blinking behavior. By contrast, for the second type of QDs, these nanoparticles exhibited relatively continuous emission without long-lived dark states. In addition, their fluorescence intensity is usually lower than that of the on-state of the blinking QDs. The phenomenon has been observed by coating single colloidal QDs on smooth Au surface. To understand the underlying mechanism of such modified blinking behavior, we performed time-resolved fluorescence measurements for these two types of QDs that exhibited distinct decay behavior even on the same ITO substrates. Fig. 17 shows that for blinking QDs, a pure single decay profile with ~11 ns lifetime was generally observed upon subtracting the background noise. On the other hand, for QDs with relatively continuous emission, we observed much faster decay dynamics with an averaged lifetime of ~3 ns. Therefore, we suggest that the modification of blinking behavior is related to the change of the fluorescence decay processes.

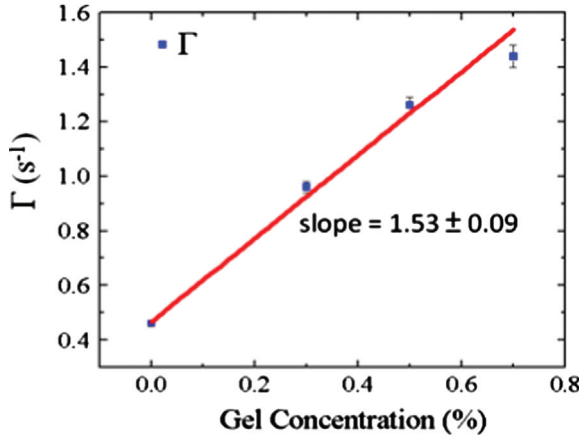

Fig. 14. Fitted exponential bending rate Γ versus gel concentration.

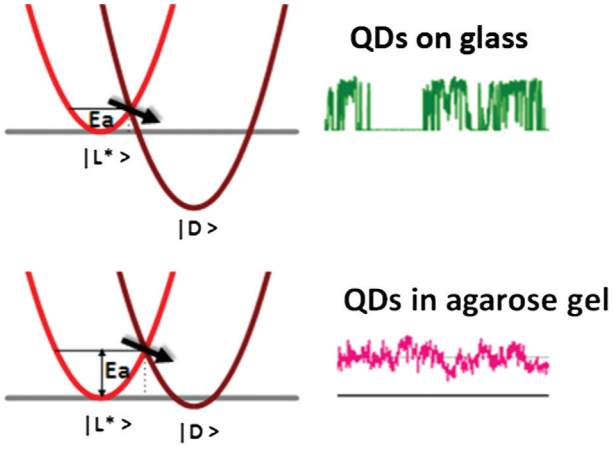

Fig. 15. The potentials for the light and dark states according to the DCET model to illustrate the influence by the changes in gel concentration.

Citation: Nano Reviews 2011, **2**: 5895 - DOI: 10.3402/nano.v2i0.5895

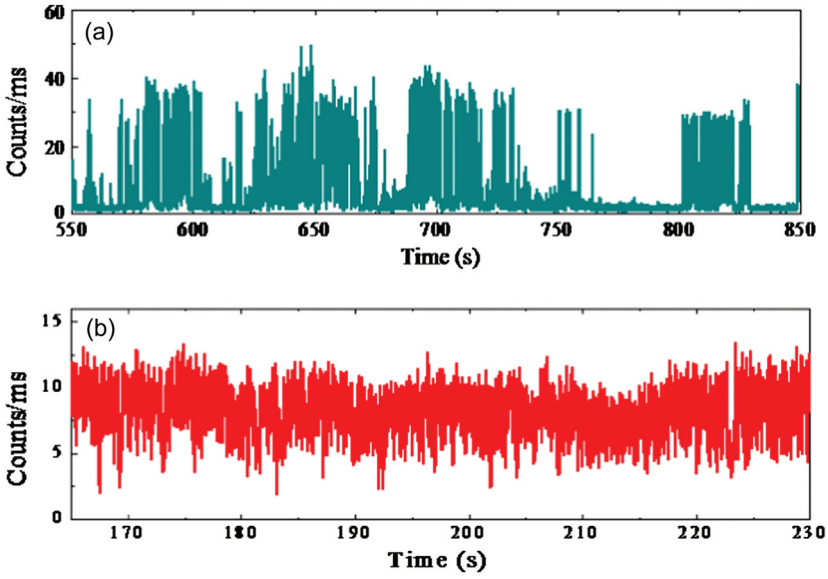

Fig. 16. Fluorescence time traces for two distinctive types of QDs, one exhibiting typical on-off blinking behavior and the other displaying a non-blinking pattern.

A previous report demonstrated that extra efficient energy transfer processes could prevail over Auger recombination to prevent QDs from entering dark states (71). Therefore, we suggest that dipole and image-dipole induced energy transfer from colloidal QDs to ITO conductive substrates could be used to explain our experimental observation including reduced fluorescence intensity, shortened fluorescence lifetimes, and continuous emission behavior. In some cases, we observed a fraction of QDs with typical blinking behavior on the same substrate. Moreover, their fluorescence characteristics are similar to that of QDs on insulating glass substrates. Therefore, we suggest that there is no interaction between QDs and ITO substrate in that situation. We performed photon correlation measurements based on Habury Brown Twiss experimental setup in order to monitor the photon statics. As shown in Fig. 18a and b, the second-order autocorrelation function for typical blinking QDs and continuous emission QDs are different indeed. For blinking QDs, photon anti-bunching behavior was observed indicating their single-photon emission characteristic. On the contrary, for less blinking QDs such typical behavior had disappeared. Here, the possibility of QD aggregation was excluded because aggregation of QDs would increase fluorescence intensity rather than quenched. Moreover, their fluorescence lifetimes should be similar to those of single QDs.

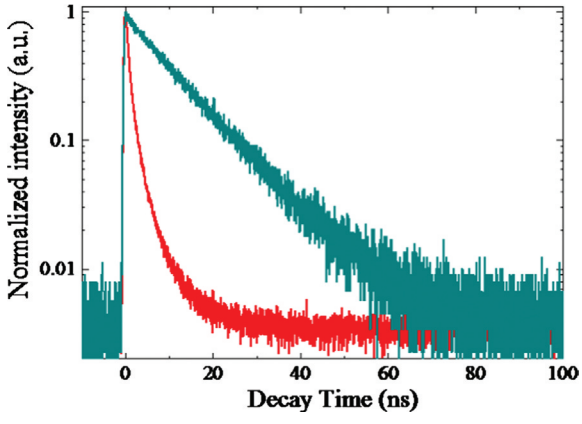

Fig. 17. Fluorescence decay curves for two distinctive types of QDs, with one showing a normal and slow decay and another showing a much faster decay.

In general, ITO is a solid solution comprised of 90% In_2O_3 and 10% SnO_2 by weight and was deposited on glass by spin coating directly. We believed that surface heterogeneity is unavoidable and it would cause distinct nano-scaled environmental changes around QDs, thus resulting in different blinking behavior. At present, the exact mechanism is still under investigation and further experiments will be needed.

Blinking suppression by reducing Auger recombination

It has long been believed that the dark states for fluorescence blinking could be attributed to the formation of positively charged QDs (45). In this case, the exciton energy is transferred to excess charges via efficient Auger recombination. For nanometer-sized nanostructures, the Auger relaxation process is more efficient than that of their bulk counterparts, owing to the breaking of the momentum conservation by quantum confinement as

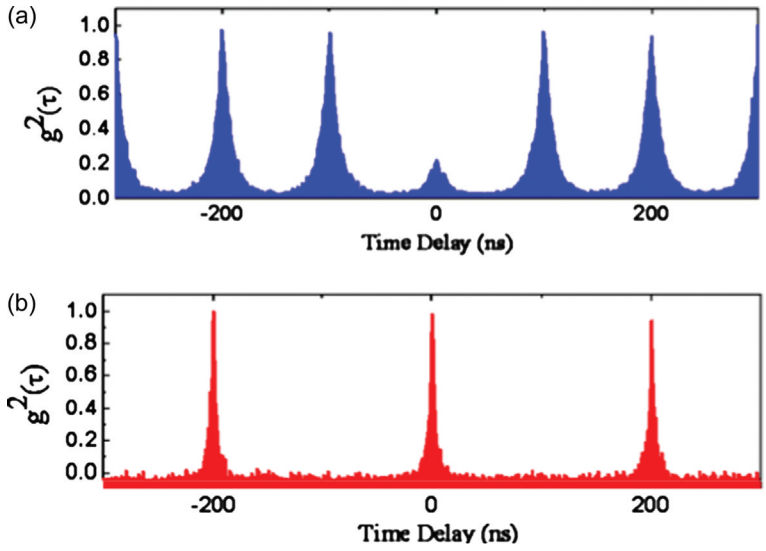

Fig. 18. Results from photon correlation measurements showing (a) anti-bunching behavior (blue curve) for blinking QDs, in comparison with (b) absence of anti-bunching (red curve) for non-blinking QDs.

reported recently (72, 73). Roughly speaking, such an Auger process is ~2 orders of magnitude faster than the radiative recombination of the neutral excitons (74). As a result, fluorescence blinking can be suppressed by Auger recombination. Actually, Auger recombination is a kind of long range Coulomb interaction and the Auger rates depend on particle sizes, shape, electronic band structures, and quantum confinements (74–77). Thus, it provides an opportunity to reduce annoying blinking behavior by modifying these physical parameters.

The general way to suppress blinking is to synthesize colloidal core/shell QDs with staggered band alignment, usually referred to as type-II QDs, exhibiting relatively weak quantum confinements due to the spatial separation between electrons and holes (78). This system can be comprised of CdSe core with CdS shell or CdTe core with CdSe shell. If Auger recombination could be reduced to be comparable with the radiative process for charged excitons, their fluorescence time trajectories would exist at gray state indicating the charged QDs are no longer dark but with distinct lifetimes with respect to neutral excitons (79). Recently, Wang et al. has synthesized novel colloidal QDs with gradient band alignment, which can display non-blinking behavior (80). Indeed, theoretical work proves that QDs with smooth potential profiles can have a weak Auger process (77).

Such a QD with weak Auger process is beneficial especially for applications in photovoltaic. In this respect, type-II band alignment can facilitate charge transfer from QDs to charge acceptors. In contrast, for conventional type-I QDs, no charge transfer could occur when QDs stayed on the off-states, owing to exciton annihilation via efficient Auger recombination. However, type-II QDs with less wave-function overlap between electrons and holes could lead to longer radiative lifetime and lower quantum yields compared with type-I counterparts. It would degrade their practical performance, in particular, as single photon sources.

Blinking suppression by enhancing radiative decay rates

In order to preserve the advantages of type-I structures and concurrently suppress unwanted fluorescence blinking, one can directly enhance radiative decay rates to prevail over Auger recombination. According to Purcell effects, the spontaneous emission rate depends not only on inherent dipole moments of light sources but also on surrounding photonic density of states. Thus, it provides an opportunity to externally control the radiative decay processes by altering photonic modes around light sources. In order to achieve this goal, the light sources can be coupled to either plasmonic or photonic modes.

Surface plasmon polaritons (SPP) are kinds of electron density waves, existing at metal-dielectric interfaces. Their electromagnetic energy is strongly confined within the sub-wavelength region. If surface plasmon is generated within the metallic nanoparticles, it cannot propagate, thus it is referred to as localized surface plasmons or particle plasmons. When light sources are placed in the proximity of metallic nanoparticles, the complex interaction could be introduced including energy transfer and excitation of localized surface plasmons. In order to optimize fluorescence intensity, a spacer layer with ~10 nm thickness can be inserted, thus minimizing energy transfer and selectively exploiting surface plasmons (66). Upon coupling to surface plasmon modes, fluorescence properties can be dramatically modified including fluorescence intensity, fluorescence lifetimes, and spatial radiation pattern.

To generate localized surface plasmons we synthesized silver nano-prisms with ~50 nm length as shown in

Citation: Nano Reviews 2011, **2**: 5895 - DOI: 10.3402/nano.v2i0.5895

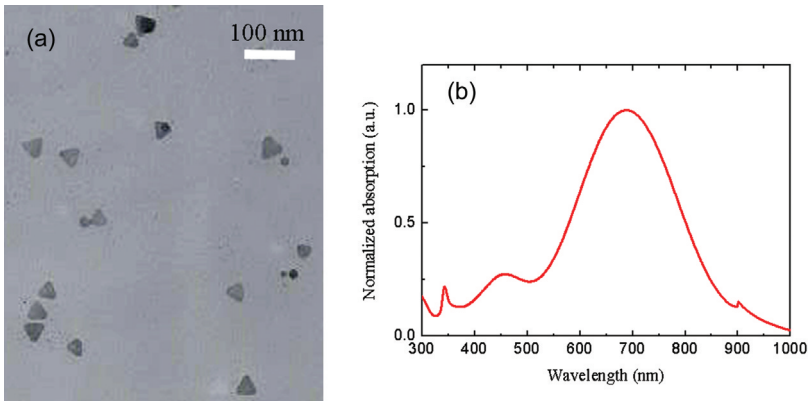

Fig. 19. (a) TEM imaging of silver nano-prisms, (b) corresponding extinction spectrum.

Fig. 19a and corresponding extinction spectra in Fig. 19b. To avoid direct energy transfer from single QDs to silver nano-prisms, a polymethyl methacrylate (PMMA) spacer layer was introduced between them. Fig. 20a and b show the fluorescence lifetime imaging for single colloidal CdSe/ZnS QDs (emission peak at ~605 nm) deposited on either pure glass or on glass further covered with silver nano-prisms (a spacer PMMA layer of ~10 nm was inserted). Obviously, a streaky pattern due to fluorescence switching can be found for single QDs on pure glass. On the contrary, a complete fluorescence spot can be seen for single QDs coupled to Ag nano-prisms. In addition, fluorescence lifetimes for pure single QDs exhibited much fluctuation with fluorescence intensity, which was attributed to the fluctuation of non-radiative decay rates (67). For QDs coupled to Ag nano-prisms, most QDs displayed blue colors indicating a shortening of their fluorescence lifetimes.

To further unravel this issue, fluorescence time trajectories of single QDs with and without coupling to silver nano-prisms are shown in Fig. 21. Indeed, fluorescence time trajectories for coupled single QDs exhibited unusual continuous emission under 10 ms bin time condition (magenta curve). Moreover, a ~2.5-fold fluorescence enhancement was found compared with pure QDs (cyan curve) for compiling more than 30 coupled QDs. Fig. 22 displays corresponding fluorescence decay profiles for single QDs with and without coupling to Ag nano-prisms. When single QDs coupled to Ag nano-prisms, their fluorescence lifetime was decreased dramatically from ~25 ns to ~5 ns.

The measured fluorescence lifetimes are determined via both radiative and non-radiative decay components, which can be described by $1/\tau_{measured} = \Gamma_{radiative} + k_{nonradiative}$. By comparing the experimental results on single QDs with and without coupling to Ag nano-prisms, one can deduce that the enhancement on the radiative decay rates is ~12.5-fold (according to the formula, $QY_{QDs-Ag}/QY_{QDs}\Gamma_{QDs-Ag}/\Gamma_{QDs} \times \tau_{QD-Ag}/\tau_{QDs}$). However, the radiative decay rates can be accelerated to the values ~12.5-fold, only 2.5-fold fluorescence enhancement was achieved, owing to unavoidable non-radiative energy transfer, thus compromised the radiative contribution.

As shown in Fig. 23, such a plasmonic quantum light source possesses unique advantages, for example, enhanced single-photon generation rates, suppressed blinking behavior, and shortened radiative lifetimes for single-photon generation. The main drawback is the residual peak at zero time delay in second-order auto-

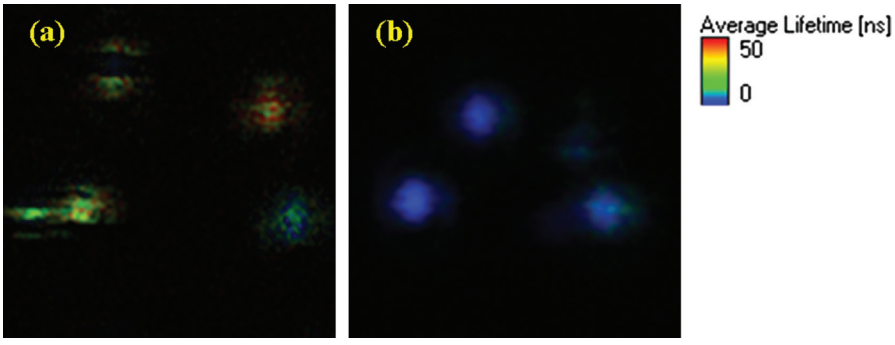

Fig. 20. Fluorescence lifetime imaging of single colloidal CdSe/ZnS QDs on either (a) pure glass or (b) on nano-prism coated glass with an embedded PMMA spacer layer of ~10 nm in thickness.

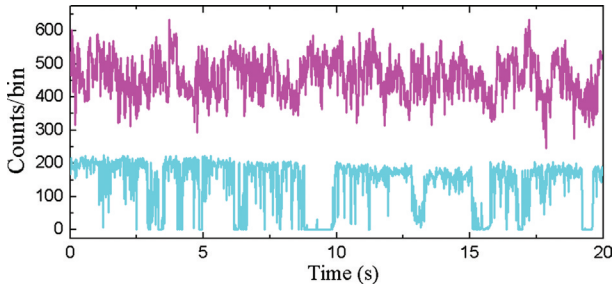

Fig. 21. Fluorescence time trajectories of single colloidal CdSe/ZnS QDs with (magenta curve) and without (cyan curve) coupling to silver nano-prisms.

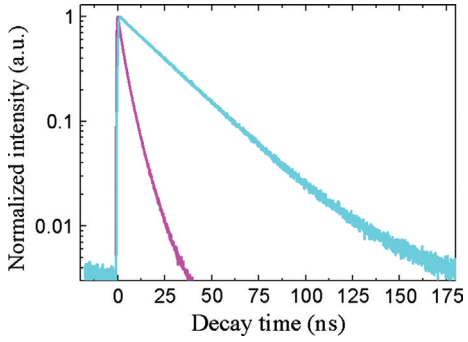

Fig. 22. Fluorescence decay profiles of single colloidal CdSe/ZnS QDs with (magenta curve) and without (cyan curve) coupling to silver nano-prisms.

correlation function, implying non-pure single-photon emission (there are some probabilities to generate more than one photon). This non-pure single-photon emission might be attributed to plasmonic emission from metallic nanostructures. Fortunately, such emission exhibits much faster decay time compared with that of most fluorophores, thus can be eliminated by post-treatment based on time-gated methods to separate fluorescence and background photons.

Blinking suppression by introducing extra energy transfer processes

The energy transfer process can occur when one dipole emitter is resonant with the other under certain conditions, for example, overlap of absorption and emission and tiny separation leading to energy flow from energy donors to acceptors. Such a process strongly depends on the relative separation between donors and acceptors. Therefore, when single colloidal QDs are placed directly onto the metallic surface, the exciton energy could be efficiently transferred to the induced image dipoles, leading to annihilation of both electrons and holes, simultaneously. Thus, upon energy transfer, the QDs would stay on the neutral states (on periods), competing with the formation of the charge separated states (dark periods), thus leading to blinking suppression (81).

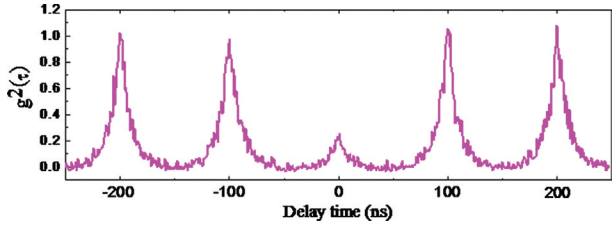

Fig. 23. Second-order autocorrelation function of single colloidal CdSe/ZnS QDs coupled to silver nano-prisms obtained by pulsed laser excitation.

As an example, Fig. 24 revealed fluorescence time trajectories of single colloidal QDs directly deposited on Ag nano-prism coated glass (red curve). For comparison, typical single-QD blinking on glass was also shown (black curve). Clearly, the on/off blinking behavior disappeared and corresponding fluorescence intensity was quenched. Recently, Chen et al., also observed similar blinking suppression for single QDs deposited on grapheme (82). In general, there existed two main interactions between light sources and metallic nano-materials (here single QDs and Ag nano-prisms). One is an energy transfer process, which caused energy transfer from single QDs to Ag nano-prisms by dipole-dipole like interaction. The other is the excitation of localized surface plasmon resonance (LSPR) by either pumping sources or QD emission. Both interactions are sensitive to the separation of QDs and Ag nano-prisms. When colloidal QDs were placed directly onto the Ag nano-prisms coated substrate, energy transfer is dominated. In contrast, when a spacer layer with about 10 to 20 nm was inserted, the LSPR contribution prevails over the energy transfer process. Therefore, we utilized a PMMA polymer as a spacer layer. By controlling PMMA concentration and spin speed, the thickness of PMMA can be tuned.

Blinking suppression by donation of excess electrons to QDs

Lately, some interesting results on blinking suppression via introducing electron donors, for example, doping substrates or reducing agents were observed (70, 83). In this case, the formation of negatively charged QDs via removing hole (either directly transferring holes or neutralizing holes) is likely a key point for blinking suppression. In general, surface passivation by donating electrons was used to explain such blinking suppression. However, some experimental observations could not be simply rationalized by only surface passivation models including quenched fluorescence intensity and shortened fluorescence lifetimes (84, 85). Therefore, apart from surface passivation, the donating electrons should play another role in determining single-QD fluorescence properties.

Fig. 25 displayed typical fluorescence decay profiles under different excitation powers for single CdSe/ZnS

Citation: Nano Reviews 2011, **2**: 5895 - DOI: 10.3402/nano.v2i0.5895

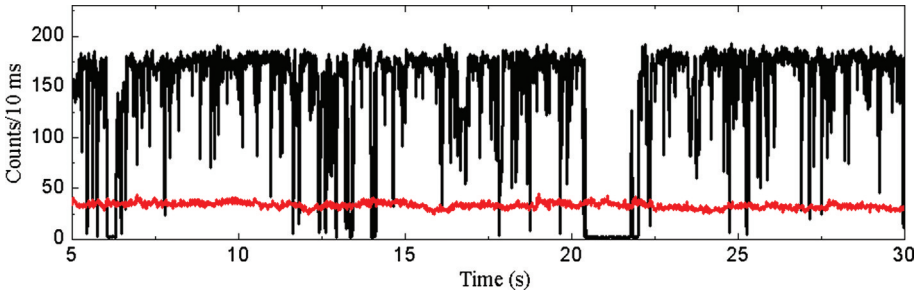

Fig. 24. Fluorescence time trajectories of single colloidal CdSe/ZnS QDs directly deposited on silver nano-prisms.

QDs in the proximity of electron donating species (DTT reducing agents). Under low-power excitation regime (less than one exciton within the QDs generated by a single laser pulse), the decay profiles can be fitted by the summation of two exponential components with ~3 ns and ~20 ns lifetimes. Here, the shorter lifetime component is assigned to the emission from negatively charged trion states (one exciton+one electron). In general, the neutral exciton has longer lifetime ~20 ns due to the existence of the lowest dark exciton states. However, no such limitation is applied to the charged excitons, thus they can decay more rapidly. For conventionally used QDs, the charged excitons with extra holes delocalized within the QDs can not emit photons owing to efficient Auger recombination. Nevertheless, for colloidal QDs with negative charges, the Auger process could be reduced, thus the radiative emission of negative trions can compete with Auger recombination, leading to relatively continuous emission.

Summary

In summary, in this review we have described some background of the progress in experiments and theoretical modeling with regard to the blinking phenomenon itself, probing the underlying mechanisms, and controlling blinking. We presented some approaches proposed by us and also by others to influence the electron transfer processes between the light and the dark states and to affect Auger relaxation processes so that one could suppress blinking behavior, partially or even completely.

To be more specific on the theoretical modeling part, we have addressed in this review the DCET model for both normal and anomalous diffusion to account for some experimental results. These issues we have addressed include single particle versus ensemble behavior, the causes of inverse power-law intermittency, and quasi-stretched exponential fluorescence intensity decay for a QD ensemble. Using the DCET model for both normal and anomalous diffusion, we have examined the relationship between the blinking behavior, $P(t)$, for single QDs and the ensemble-averaged fluorescence decay, $\langle I(t)\rangle$. We have also elucidated the relationship between $\langle I(t)\rangle$ and relaxation function $\langle R(t)\rangle$ with $P_k(t)$. All these time profiles $\langle I(t)\rangle$, $\langle R(t)\rangle$ and $P(t)$ follow characteristically different decaying behavior during various time regimes. From the measurements of single-particle or ensemble behavior, one can in principle extract those molecular-based quantities.

Other than elucidating the blinking mechanisms, moreover, we have presented our recent investigation of the environmental effects on the blinking behavior of QDs such as encapsulating a single QD inside nano- to micron-sized pores of agarose gel or spin-coating QDs on various substrates. We have also discussed several approaches to suppress blinking as demonstrated in our recent work or other groups. These approaches include reducing the Auger relaxation rate, enhancing radiative decay rate, and so on. With better control of blinking behavior and complete suppression of blinking, these QDs could become more practical as light sources in

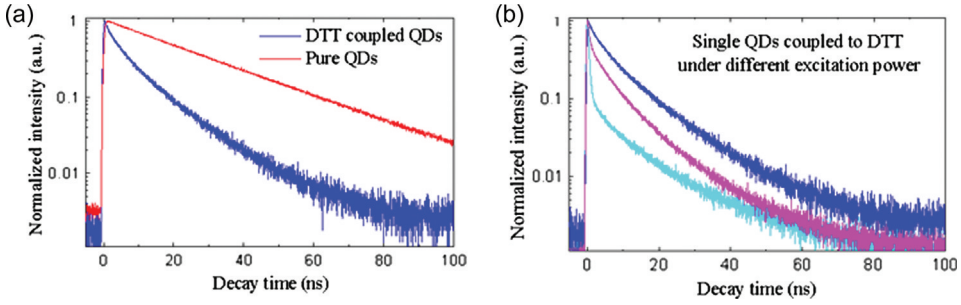

Fig. 25. (a) Fluorescence decay profiles for single CdSe/ZnS QDs with and without coupling to DTT reductants. (b) Power-dependent fluorescence decay profiles for DTT-coupled single QDs. The excitation intensities for three curves are 1000 nW (denoted as high power), 400 nW (denoted as intermediate power), and 100 nW (denoted as low power), respectively.

optoelectronic applications or fluorescence labels in biomedical imaging applications.

Acknowledgements

We acknowledge the support of the Academia Sinica and National Science Council of Taiwan under the program No.99-2113-M-001-023-MY3.

Conflict of interest and funding

There is no conflict of interest in the present study for any of the authors.

References

1. Jacak L, Hawrylak P, Wojs A. Quantum dots. Berlin: Springer; 1997.
2. Heiss WD, ed. Quantum dots: a doorway to nanoscale physics. Berlin: Springer; 2005.
3. Botell V, ed. Nanoparticles: building blocks for nanotechnology. New York: Kluwer Academic; 2004.
4. Parak WJ, Pellegrino T, Plank C. Labelling of cells with quantum dots. Nanotechnology 2005; 16: R9–R25.
5. Hammer PW, Platt N, Hammel SM, Heagy JF, Lee BD. Experimental observation of on-off intermittency. Phys Rev Lett 1994; 73: 1095–8.
6. Osad'ko IS. Model for power-law statistics in blinking photoluminescence of single semiconductor nanocrystals. Chem Phys 2005; 316: 99–107.
7. Zusman LD. Outer-sphere electron-transfer in polar-solvents. Chem Phys 1980; 49: 295–304.
8. Sumi H, Marcus RA. Dynamic effects in electron-transfer reactions. J Chem Phys 1986; 84: 4894–914.
9. Rips I, Jortner J. Outer sphere electron-transfer in polar-solvents – activationless and inverted regimes. J Chem Phys 1987; 87: 6513–9.
10. Yan YJ, Sparpaglione M, Mukamel S. Solvation dynamics in electron-transfer, isomerization, and nonlinear optical processes – a unified liouville-space theory. J Phys Chem 1988; 92: 4842–53.
11. Seki K, Barzykin AV, Tachiya M. Diffusion-assisted long-range reactions in confined systems: projection operator approach. J Chem Phys 1999; 110: 7639–49.
12. Bicout DJ, Szabo A. Electron transfer reaction dynamics in non-Debye solvents. J Chem Phys 1998; 109: 2325–38.
13. Bouchaud JP, Georges A. Anomalous diffusion in disordered media – statistical mechanisms, models and physical applications. Phys Rep 1990; 195: 127–293.
14. Hynes JT. Outer-sphere electron-transfer reactions and frequency-dependent friction. J Phys Chem 1986; 90: 3701–6.
15. Renger T, Marcus RA. On the relation of protein dynamics and exciton relaxation in pigment-protein complexes: an estimation of the spectral density and a theory for the calculation of optical spectra. J Chem Phys 2002; 116: 9997–10019.
16. Böttcherm CJF, Bordewijk P. Theory of electric polarization, vol. II. Amsterdam: Elsevier; 1978.
17. Nirmal M, Dabbousi BO, Bawendi MG, Macklin JJ, Trautman JK, Harris TD, et al. Fluorescence intermittency in single cadmium selenide nanocrystals. Nature 1996; 383: 802–4.
18. Kuno M, Fromm DP, Hamann HF, Gallagher A, Nesbitt DJ. Nonexponential 'blinking' kinetics of single CdSe quantum dots: a universal power law behavior. J Chem Phys 2000; 112: 3117–20.
19. Cao JS. Effects of bath relaxation on dissipative two-state dynamics. J Chem Phys 2000; 112: 6719–24.
20. Tang J, Marcus RA. Diffusion-controlled electron transfer processes and power-law statistics of fluorescence intermittency of nanoparticles. Phys Rev Lett 2005; 95: 107401–1 to 107401–4.
21. Krauss TD, Brus LE. Charge, polarizability, and photoionization of single semiconductor nanocrystals. Phys Rev Lett 1999; 83: 4840–3.
22. Krauss TD, O'Brien S, Brus LE. Charge and photoionization properties of single semiconductor nanocrystals. J Phys Chem B 2001; 105: 1725–33.
23. Nirmal M, Norris DJ, Kuno M, Bawendi MG, Efros AL, Rosen M. Observation of the dark exciton in CdSe quantum dots. Phys Rev Lett 1995; 75: 3728–31.
24. Empedocles SA, Bawendi MG. Influence of spectral diffusion on the line shapes of single CdSe nanocrystallite quantum dots. J Phys Chem B 1999; 103: 1826–30.
25. Shimizu KT, Neuhauser RG, Leatherdale CA, Empedocles SA, Woo WK, Bawendi MG. Blinking statistics in single semiconductor nanocrystal quantum dots. Phys Rev B 2001; 63: 205316.
26. Shimizu KT, Woo WK, Fisher BR, Eisler HJ, Bawendi MG. Surface-enhanced emission from single semiconductor nanocrystals. Phys Rev Lett 2002; 89: 117401.
27. Chung IH, Bawendi MG. Relationship between single quantum-dot intermittency and fluorescence intensity decays from collections of dots. Phys Rev B 2004; 70: 165304.
28. Fisher BR, Eisler HJ, Stott NE, Bawendi MG. Emission intensity dependence and single-exponential behavior in single colloidal quantum dot fluorescence lifetimes. J Phys Chem B 2004; 108: 143–8.
29. Chung I, Witkoskie JB, Cao J, Bawendi MG. Description of the fluorescence intensity time trace of collections of CdSe nanocrystal quantum dots based on single quantum dot fluorescence blinking statistics. Phys Rev E 2006; 73: 011106.
30. Kuno M, Fromm DP, Hamann HF, Gallagher A, Nesbitt DJ. 'On'/'off' fluorescence intermittency of single semiconductor quantum dots. J Chem Phys 2001; 115: 1028–40.
31. Kuno M, Fromm DP, Johnson ST, Gallagher A, Nesbitt DJ. Modeling distributed kinetics in isolated semiconductor quantum dots. Phys Rev B 2003; 67: 125304.
32. Messin G, Hermier JP, Giacobino E, Desbiolles P, Dahan M. Bunching and antibunching in the fluorescence of semiconductor nanocrystals. Opt Lett 2001; 26: 1891–3.
33. Brokmann X, Hermier JP, Messin G, Desbiolles P, Bouchaud JP, Dahan M. Statistical aging and nonergodicity in the fluorescence of single nanocrystals. Phys Rev Lett 2003; 90: 120601.
34. Verberk R, van Oijen AM, Orrit M. Simple model for the power-law blinking of single semiconductor nanocrystals. Phys Rev B 2002; 66: 233202.
35. Verberk R, Orrit M. Photon statistics in the fluorescence of single molecules and nanocrystals: Correlation functions versus distributions of on- and off-times. J Chem Phys 2003; 119: 2214–22.
36. Cichos F, Martin J, von Borczyskowski C. Emission intermittency in silicon nanocrystals. Phys Rev B 2004; 70: 115314.
37. Issac A, von Borczyskowski C, Cichos F. Correlation between photoluminescence intermittency of CdSe quantum dots and self-trapped states in dielectric media. Phys Rev B 2005; 71: 161302.
38. Schlegel G, Bohnenberger J, Potapova I, Mews A. Fluorescence decay time of single semiconductor nanocrystals. Phys Rev Lett 2003; 88: 137401.

Citation: Nano Reviews 2011, **2**: 5895 - DOI: 10.3402/nano.v2i0.5895

39. Pelton M, Grier DG, Guyot-Sionnest P. Characterizing quantum-dot blinking using noise power spectra. Appl Phys Lett 2004; 85: 819–21.
40. Labeau O, Tamarat P, Lounis B. Temperature dependence of the luminescence lifetime of single CdSe/ZnS quantum dots. Phys Rev Lett 2003; 90: 257404.
41. Biju V, Makita Y, Nagase T, Yamaoka Y, Yokoyama H, Baba Y, et al. Subsecond luminescence intensity fluctuations of single CdSe quantum dots. J Phys Chem B 2005; 109: 14350–5.
42. Frantsuzov P, Kuno M, Janko B, Marcus RA. Universal emission intermittency in quantum dots, nanorods and nanowires. Nature Physics 2008; 4: 519–22.
43. Haase M, Hubner CG, Reuther E, Herrmann A, Mullen K, Basche T. Exponential and power-law kinetics in single-molecule fluorescence intermittency. J Phys Chem B 2004; 108: 10445–50.
44. Schuster J, Cichos F, von Borczyskowski C. Influence of self-trapped states on the fluorescence intermittency of single molecules. Appl Phys Lett 2005; 87: 051915.
45. Efros AL, Rosen M. Random telegraph signal in the photoluminescence intensity of a single quantum dot. Phys Rev Lett 1997; 78: 1110–3.
46. Wang J, Wolynes P. Intermittency of activated events in single molecules: the reaction diffusion description. J Chem Phys 1999; 110: 4812–9.
47. Boguna M, Berezhkovskii AM, Weiss GH. Residence time densities for non-Markovian systems. (I). The two-state system. Physica A 2000; 282: 475–85.
48. Barkai E, Jung Y, Silbey R. Theory of single-molecule spectroscopy: Beyond the ensemble averag Annu. Rev. Phys. Chem. 2004; 55: 457–507.
49. Margolin G, Barkai E. Aging correlation functions for blinking nanocrystals, and other on-off stochastic processes. J Chem Phys 2004; 121: 1566–77.
50. Tang J, Marcus RA. Mechanisms of fluorescence blinking in semiconductor nanocrystal quantum dots. J Chem Phys 2005; 123: 054704.
51. Tang J, Marcus RA. Single particle versus ensemble average: from power-law intermittency of a single quantum dot to quasistretched exponential fluorescence decay of an ensemble. J Chem Phys 2005; 123: 204511.
52. Frantsuzov PA, Marcus RA. Explanation of quantum dot blinking without the long-lived trap hypothesis. Phys Rev B 2005; 72: 155321.
53. Flomenbom O, Klafter J, Szabo A. What can one learn from two-state single-molecule trajectories? Biophys J 2005; 88: 3780–3.
54. Tang J. Fluorescence intermittency of silicon nanocrystals and other quantum dots: a unified two-dimensional diffusion-controlled reaction model. J Chem Phys 2007; 127: 111105.
55. Tang J, Lee DH, Yeh YC, Yuan CT. Short-time power-law blinking statistics of single quantum dots and a test of the diffusion-controlled electron transfer model. J Chem Phys. 2009; 131: 064506.
56. Alvarez F, Alegria A, Colmenero J. Relationship between the time-domain Kohlrausch-Williams-Watts and frequency-domain Havriliak-Negami relaxation functions. Phys Rev B 1991; 44: 7306–12.
57. Tang J. The effects of anomalous diffusion on power-law blinking statistics of CdSe nanorods. J Chem Phys 2008; 129: 084709.
58. Tang J. Size effects and breakdown of the power-law blinking statistics of CdSe nanorods. J Phys Chem A 2007; 111: 9336–9.
59. Yeh YC, Yuan CT, Kang CC, Chou PT. Influences of light intensity on fluorescence lifetime of nanorods and quantum dots. Appl Phys Lett 2008; 93: 223110.
60. Bardou F, Bouchaud JP. Aspect A, Cohen-Tannoudji C. Lévy Statistics and Laser Cooling. England: Cambridge 2001.
61. Ko HC, Yuan CT, Lin SH, Tang J. Blinking suppression of single quantum dots in agarose gel. Appl Phys Lett 2010; 96: 012104.
62. Maaloum M, Pernodet N, Tinland B. Agarose gel structure using atomic force microscopy: gel concentration and ionic strength effects. Electrophoresis 1998; 19: 1606–10.
63. Stellwagen NC, Gelfi C, Righetti PG. DNA and buffers: the hidden danger of complex formation. Biopolymers 2000; 54: 137–42.
64. Serwer P, Hayes SJ. Agarose-gel electrophoresis of bacteriophages and related particles. 1. Avoidance of binding to the gel and recognizing of particles with packaged DNA. Electrophoresis 1982; 3: 76–80.
65. Serwer P. Agarose gels – properties and use for electrophoresis. Electrophoresis 1983; 4: 375–82.
66. Yuan CT, Yu P, Ko HC, Huang J, Tang J. Antibunching single-photon emission and blinking suppression of CdSe/ZnS quantum dots. ACS Nano 2009; 3: 3051–6.
67. Wu XW. Anti-bunching and luminescence blinking suppression from plasmon-interacted single CdSe/ZnS quantum dot. Opt Express 2010; 18: 6340–6.
68. Fu Y, Zhang J, Lakowicz JR. Silver-enhanced fluorescence emission of single quantum dot nanocomposites. Chem Comm 2009; 3: 313–5.
69. Masuo S, Naiki H, Machida S, Itaya A. Photon statistics in enhanced fluorescence from a single CdSe/ZnS quantum dot in the vicinity of silver nanoparticles. Appl Phys Lett 2009; 95: 193106.
70. Jin SY, Song NH, Lian TQ. Suppressed blinking dynamics of single QDs on ITO. Acs Nano 2010; 4: 1545–52.
71. Hamada M, Nakanishi S, Itoh T, Ishikawa M, Biju V. Blinking suppression in CdSe/ZnS single quantum dots by TiO2 nanoparticles. ACS Nano 2010; 4: 4445–54.
72. Zhao J, Nair G, Fisher BR, Bawendi MG. Challenge to the charging model of semiconductor-nanocrystal fluorescence intermittency from off-state quantum yields and multiexciton blinking. Phys Rev Lett 2010; 104: 157403.
73. Rosen S, Schwartz O, Oron D. Transient fluorescence of the off state in blinking CdSe/CdS/ZnS semiconductor nanocrystals is not governed by auger recombination. Phys Rev Lett 2010; 104: 157404.
74. Klimov VI, Mikhailovsky AA, McBranch DW, Leatherdale CA, Bawendi MG. Quantization of multiparticle auger rates in semiconductor quantum dots. Science 2000; 287: 1011–3.
75. Robel I, Gresback R, Kortshagen U, Schaller RD, Klimov VI. Universal size-dependent trend in auger recombination in direct-gap and indirect-gap semiconductor nanocrystals. Phys Rev Lett 2009; 102: 177404.
76. Garcia-Santamaria F, Chen YF, Vela J, Schaller RD, Hollingsworth JA, Klimov VI. Suppressed auger recombination in 'giant' nanocrystals boosts optical gain performance. Nano Lett 2009; 9: 3482–8.
77. Cragg GE, Efros AL. Suppression of auger processes in confined structures. Nano Lett 2010; 10: 313–7.
78. Mahler B, Spinicelli P, Buil S, Quelin X, Hermier JP, Dubertret B. Towards non-blinking colloidal quantum dots. Nat Mater 2008; 7: 659–64.
79. Spinicelli P, Buil S, Quelin X, Mahler B, Dubertret B, Hermier JP. Bright and grey states in CdSe-CdS nanocrystals exhibiting strongly reduced blinking. Phys Rev Lett 2009; 102: 136801.
80. Wang XY, Ren XF, Kahen K, Hahn MA, Rajeswaran M, Maccagnano-Zacher S, et al. Non-blinking semiconductor nanocrystals. Nature 2009; 459: 686–9.

81. Yuan CT, Yu P, Tang J. Blinking suppression of colloidal CdSe/ZnS quantum dots by coupling to silver nanoprisms. Appl Phys Lett 2009; 94: 243108.
82. Chen ZY, Berciaud S, Nuckoll C, Heinz TF, Brus LE. Energy transfer from individual semiconductor nanocrystals to graphene. ACS Nano 2010; 4: 2964–8.
83. Hohng S, Ha T. Near-complete suppression of quantum dot blinking in ambient conditions. J Am Chem Soc 2004; 126: 1324–5.
84. Antelman J, Ebenstein Y, Dertinger T, Michalet X, Weiss S. Suppression of quantum dot blinking in DTT-doped polymer films. J Phys Chem C 2009; 113: 11541–5.
85. Fomenko V, Nesbitt DJ. Solution control of radiative and nonradiative lifetimes: a novel contribution to quantum dot blinking suppression. Nano Lett 2008; 8: 287–93.

***Chi-Tsu Yuan**
Research Center for Applied Sciences
Academia Sinica
Taipei 115, Taiwan
Email: chitsuyuan@gmail.com

***Jau Tang**
Research Center for Applied Sciences
Academia Sinica
Taipei 115, Taiwan
Email: jautang@gate.sinica.edu.tw

Citation: Nano Reviews 2011, **2**: 5895 - DOI: 10.3402/nano.v2i0.5895